Magnetic trilayers with bilinear and biquadratic exchange couplings: Criteria for the measurement of J_1 and J_2

C. Chesman,* M. A. Lucena, M. C. de Moura, A. Azevedo, F. M. de Aguiar, and S. M. Rezende
Departamento de Física, Universidade Federal de Pernambuco, 50670-901 Recife, Brazil

S. S. P. Parkin
IBM Research Division, Almaden Research Center, 650 Harry Road, San Jose, California 95120-6099
(Received 9 February 1998)

We have analytically calculated phase boundaries of magnetic trilayers with bilinear and biquadradic exchange couplings in order to investigate possible phase transitions in these systems as the external magnetic field, applied either along an easy or a hard magnetization axis, is varied. A simple scheme is obtained for both antiferromagnetic and ferromagnetic couplings that is shown to be consistent with magnetization curves previously measured in different systems. In addition, experimental data regarding static and dynamic responses in sputtered (100) Fe(40 Å)/Cr(t_{Cr})/Fe(40 Å) are reported for the Cr thickness in the range 15 Å$< t_{\mathrm{Cr}}<$35 Å. As a result, our model calculations indicate that the bilinear and biquadratic exchange coupling constants, J_1 and J_2, cannot be accurately determined from a fit to the experimental data when the ratio $J_2/|J_1|>1$, and if only the main magnetization axes are considered. [S0163-1829(98)02725-8]

Layered films of ferromagnetic metals exchange coupled through a nonferromagnetic spacer layer are of considerable fundamental and technological interest. Remarkable findings in these systems include interlayer antiferromagnetic (AF) coupling,[1] the concurrent giant magnetoresistance (GMR),[2] oscillations in the interlayer exchange coupling and GMR as a function of the spacer layer thickness,[3] and biquadratic exchange coupling.[4,5] On the other hand, magnetoelectric devices based on the GMR have been widely considered for applications in information storage technology.[6–8] The relationship between the interlayer exchange coupling and the GMR thus makes the measurement of the former of primary importance. The cheapest and most widely used technique in this regard is the magneto-optical Kerr effect (MOKE), which is useful for extracting the bilinear exchange constant only if the coupling is AF. Other techniques, such as ferromagnetic resonance (FMR) and Brillouin light scattering (BLS), are needed in the case of ferromagnetic coupling.

We have recently presented phenomenological model calculations where the coupling between the magnetic films is fully taken into account through bilinear and biquadratic exchange and magnetic dipolar interactions, together with surface, in-plane uniaxial and cubic anisotropies.[9] The calculations were previously shown to provide good quantitative agreement with MOKE, magnetoresistance, FMR, and BLS experiments in several trilayer systems,[10–12] with the advantage of treating both static and dynamic responses on an equal footing. In this report we present further investigations of phase transitions in sputtered (100) Fe/Cr/Fe trilayers exhibiting bilinear and biquadratic exchange couplings, making use of phase diagrams to help in understanding the behavior of the magnetizations as the external magnetic field is varied. Previous studies on phase diagrams either did not take into account the biquadratic interaction,[13] nor looked carefully at the so-called 90° phase,[14] where the magnetizations in the two magnetic films are nearly perpendicular to each other. As has been demonstrated previously,[10] the biquadratic interaction leads to first-order phase transitions in the magnetization's configuration, and numerical approaches are usually required to circumvent this problem. Here we show that, in simple yet usual situations, one can obtain analytical expressions for the boundaries between phases, which are quite useful in interpreting the experimental data. Since the details of our analysis may be found elsewhere,[9–12] we present here only the main assumptions aiming at the steps for obtaining the expressions for the critical fields.

We consider a very thin trilayer, so that the dipolar interaction can be neglected, and could be described in terms of a free energy per unit area $E=E_Z+E_A+E_E$, where the three terms on the right-hand side are, respectively, the Zeeman, the fourfold magneto-crystalline anisotropy, and the exchange (bilinear and biquadratic) energies. We assume that the ferromagnetic layers have the same thickness d, and that the magnetizations are uniform in both layers, with the same saturation value M_S. For the external magnetic field $\mathbf{H}_0$ applied in the film plane, this energy can be written as[9]

$$E=-\sum_{i=1}^{2}\left[H_0\cos(\theta_i-\theta_H)-\tfrac{1}{8}H_A\sin^2(2\theta_i)\right]$$
$$-H_{bl}\cos(\theta_1-\theta_2)+H_{bq}\cos^2(\theta_1-\theta_2), \qquad (1)$$

where the effective fields are given by $H_A=2K_1/M_S$ (K_1 = effective anisotropy constant), $H_{bl}=J_1/dM_S$, and $H_{bq}=J_2/dM_S$. The variables θ_H, θ_1, and θ_2 are, respectively, the angles of the applied field and of the equilibrium magnetizations with respect to an easy axis. Consider a system grown in the (100) plane, with a spacer layer thickness such that the bilinear and biquadratic interactions are of the same order of magnitude. Furthermore, assume that the external field is applied along the [001] easy magnetization axis. The equilibrium configuration can be determined by equating to zero the derivatives of the free energy with respect to the angles θ_1 and θ_2. In the case of AF coupling, there are three possible phases, namely, AF, 90°, and saturated.[10] The ex-

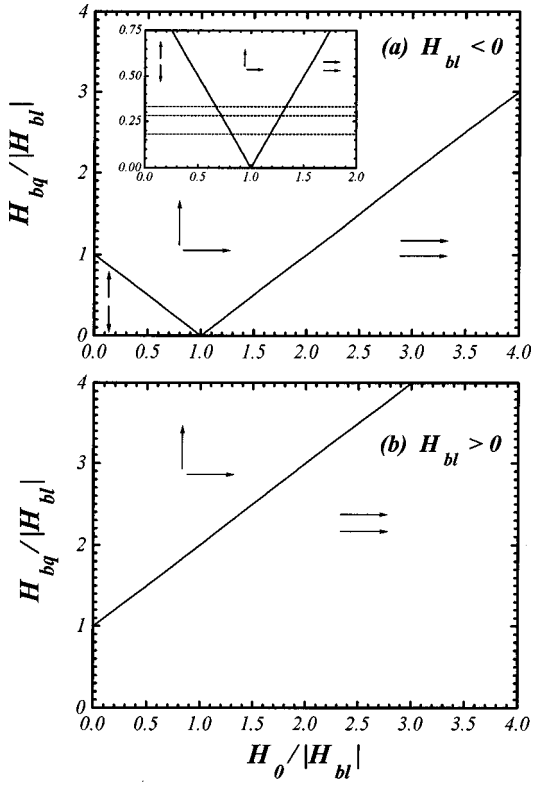

FIG. 1. Calculated phase diagram $H_{bq}/|H_{bl}|$ vs $H_0/|H_{bl}|$ for antiferromagnetic (a) and ferromagnetic (b) coupling for a symmetric thin-film trilayer. The arrows indicate the relative positions of the magnetizations in the two magnetic films in each phase. The three horizontal lines in the inset correspond, from top to bottom, to the sweep of the external magnetic field in the MOKE experiments described in Refs. 10, 16, and 17, respectively.

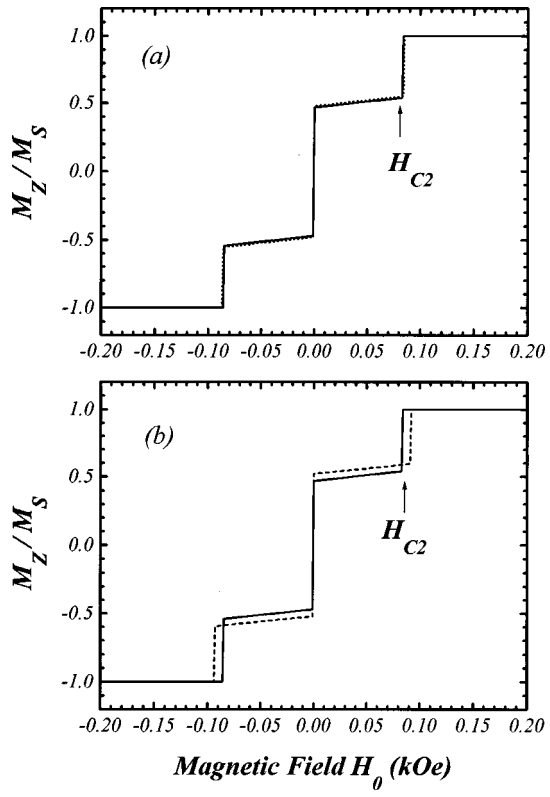

FIG. 2. (a) Calculated magnetization curve for a trilayer with $H_{bl}=-40$ Oe and $H_{bq}=+40$ Oe (solid line) and $H_{bl}=-27$ Oe and $H_{bq}=+54$ Oe (dashed line). (b) Same as (a), with $H_{bl}=-40$ Oe and $H_{bq}=+40$ Oe (solid line) and $H_{bl}=+40$ Oe and $H_{bq}=+120$ Oe (dashed line).

pression for the critical field H_{C1} that separates the AF phase from the 90° phase can be determined from the boundary condition

$$E(\theta_1=-90°,\ \theta_2=90°,\ \theta_H=0) = E(\theta_1=0,\ \theta_2=90°,\ \theta_H=0),$$

that gives

$$H_{C1}=-(H_{bl}+H_{bq}). \tag{2}$$

Actually, θ_1 and θ_2 have a weak dependence on the magnetic field within each region,[9,10] but, as far as the determination of the critical field is concerned, the values taken at the frontier are excellent approximations to the real ones. Similarly, for the boundary H_{C2} between the 90° and the saturated phases, we assume that $\theta_1=0$ and $\theta_2=90°$ in the 90° phase, while we take $\theta_1=\theta_2=0$ in the saturated one. By applying the boundary condition, we obtain the critical field

$$H_{C2}=-(H_{bl}-H_{bq}). \tag{3}$$

Notice that in this case the effective anisotropy field has no influence on H_{C1} and H_{C2}. However, it can be shown[15] that the situation described here is possible only if $H_A>2|H_{bl}|$. Thus, the transitions predicted by Eqs. (2) and (3) may not occur if the magnetic films are too thin. The boundaries given by Eqs. (2) and (3) are shown by the solid lines in the phase diagram of Fig. 1(a). One can see that if the ratio $\eta \equiv H_{bq}/|H_{bl}|=J_2/|J_1|$ is smaller than one, the values of the effective exchange fields can be determined from the measured values of H_{C1} and H_{C2} through Eqs. (2) and (3), namely, $H_{bl}=-(H_{C1}+H_{C2})/2$, and $H_{bq}=(H_{C2}-H_{C1})/2$. To illustrate the usefulness of this diagram, we show by the horizontal lines in the inset of Fig. 1(a), our classification of three magnetic-field sweeps in MOKE measurements in Fe/Cr/Fe. The uppermost line corresponds to our own result described in Ref. 10, while the mid and lower lines fit the data in Refs. 16 and 17, respectively. We show in Fig. 1(b) the phase diagram for the ferromagnetic coupling, in the same η range. In this case, there is only one transition at a critical field given by Eq. (3), if $\eta>1$. That happens when the coupling is AF and $\eta>1$, as well. Therefore, only the difference $H_{bq}-H_{bl}$ would be available from a measurement of H_{C2} in this case ($\eta>1$). There are important consequences following this restriction, to which little attention seems to have been paid. First, we point out that the authors in Refs. 18 and 19 were most probably working in this regime, and that might explain why they were unable to provide a precise measurement of both bilinear and biquadratic exchange parameters from their experiments. To better illustrate this point, we show in Fig. 2 plots of $M_Z/M_S=(\cos\theta_1+\cos\theta_2)/2$, a quantity that is proportional to the MOKE signal. The solid line in Fig. 2(a) was obtained with $H_{bl}=-40$ Oe and $H_{bq}=+40$ Oe ($\eta=1$), while the dotted line corresponds to $H_{bl}=-27$ Oe and $H_{bq}=+54$ Oe ($\eta=2$). Thus, quite different values of H_{bl}, H_{bq}, and η

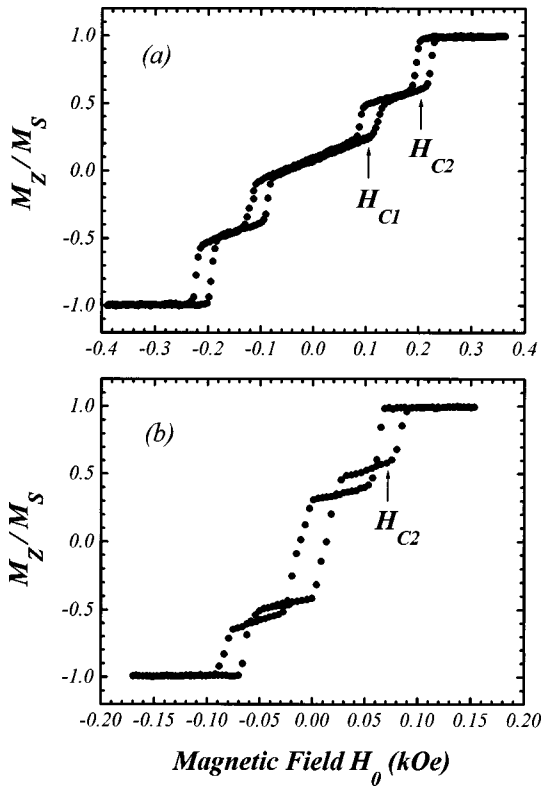

FIG. 3. MOKE data in (100) Fe(40 Å)/Cr(t_{Cr})/Fe(40 Å) for $t_{Cr}=15$ Å (a) and $t_{Cr}=25$ Å (b), as described in the text.

($\eta \geqslant 1$), can result in almost identical magnetization curves. Another ambiguous issue might happen if $\eta \geqslant 1$: as shown in Fig. 2(b), where the solid (dotted) line corresponds to $H_{bl}=-40$ Oe ($+40$ Oe) and $H_{bq}=+40$ Oe ($+120$ Oe), reasonable fits to a hypothetically measured magnetization curve could be obtained for both AF (solid line) and ferromagnetic (dotted line) coupling. Which coupling would be the right one? Finally, if $\eta \geqslant 1$, one might attempt to measure H_{bl} and H_{bq} by applying the magnetic field along the hard axis, as well. In this case, there is a second-order transition between a spin-flop and the saturated phase,[11] at the critical field $H_{C3}=-2H_{bl}+4H_{bq}+H_A$. Thus, a measurement of H_{C2} and H_{C3} would allow one to determine H_{bl} and H_{bq}, provided H_A is known. However, the fitting parameter H_A is usually much larger than H_{bq}, and it is difficult to measure H_{C3} precisely, given that this transition is of second-order nature.

In the remainder of the paper, we apply the results above to the Fe(40 Å)/Cr(t_{Cr})/Fe(40 Å) system. The samples were grown onto (100) MgO substrates by sputter deposition in a UHV chamber, and belong to the same batch as the sample with $t_{Cr}=15$ Å discussed in Ref. 10. Figure 3 shows room-temperature MOKE measurements in two representative samples located close to the first and second AF peaks,[10] namely, $t_{Cr}=15$ Å [Fig. 3(a)] and $t_{Cr}=25$ Å [Fig. 3(b)], respectively. Figure 3(a) is clearly a situation in which $\eta<1$, and the measured values of H_{C1} and H_{C2} yield $H_{bl}=-150$ Oe and $H_{bq}=50$ Oe, i.e., $\eta=0.33$, consistent with the phase diagram in Fig. 1(a). The reduced value of $|H_{bl}|$ is apparent for the sample with $t_{Cr}=25$ Å, which exhibits only the transition between the 90° and the saturated phases. In this case $\eta \geqslant 1$, and we cannot determine the two coupling fields accurately, as previously explained. Surprisingly, the same behavior were observed for all samples around the second AF peak. In Fig. 4 we show the magnetization curves observed in the samples with $t_{Cr}=29$ Å [Fig. 4(a)], 33 Å [Fig. 4(b)], and 35 Å [Fig. 3(c)], with shapes qualitatively similar to that in Fig. 3(b), and thus, with the same restriction regarding the coupling fields. We have also used the FMR and BLS techniques in some of these samples, with equally limited results. For instance, the symbols in Fig. 5 are the acoustic and optic modes in the sample with $t_{Cr}=25$ Å, as measured by BLS, with the same configuration described in Ref. 10. The solid and dashed lines are numerical fits with parameters $4\pi M_S=20.5$ kG, $H_A=0.55$ kOe, as for the sample with $t_{Cr}=15$ Å, and $\eta=1.0$ and 1.2, respectively. The fits are almost identical, in spite of the different ratios η used.

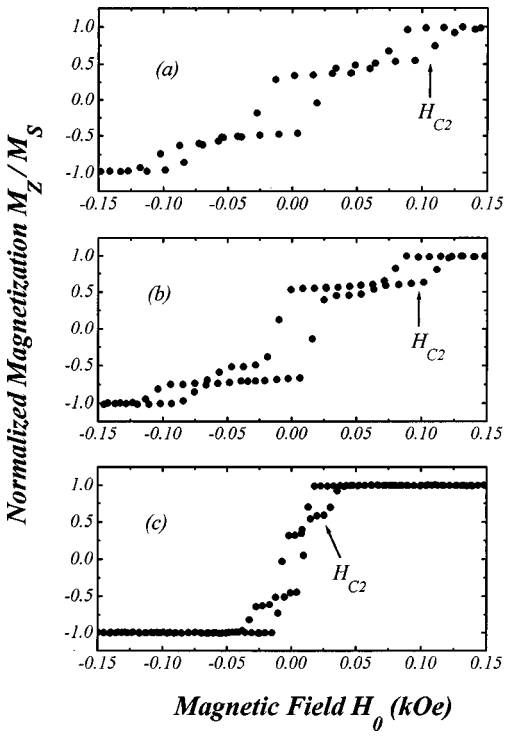

FIG. 4. Same as Fig. 3, for $t_{Cr}=29$ Å (a), 33 Å (b), and 35 Å (c).

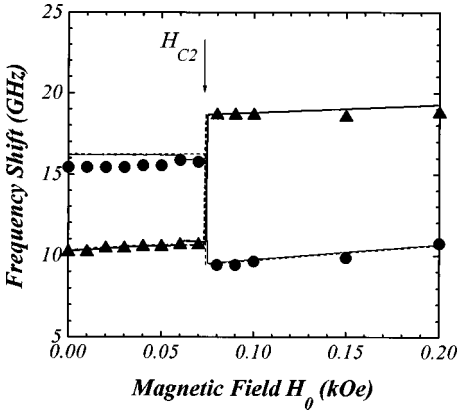

FIG. 5. Magnon frequencies for $q=1.22\times10^5$ cm^{-1} vs external field H_0, applied along an easy magnetization axis in (100) Fe(40 Å)/Cr(25 Å)/Fe(40 Å). Symbols are BLS data: circles for the optic mode and triangles for the acoustic mode. The lines are theoretical fits (Ref. 9) with $H_{bq}/|H_{bl}|=1.0$ (solid line) and 1.2 (dashed line).

We thank N. S. Almeida for valuable discussions on phase diagrams and for sending us a preprint of Ref. 15 prior to publication, and K. P. Roche for technical assistance. The work at UFPE has been supported by the Brazilian Federal Agencies CNPq, CAPES, PADCT, and FINEP, and by the Pernambuco State Agency FACEPE. The work at IBM was partially supported by the Office of Naval Research.

*Present address: Departamento de Física Teórica e Experimental, Universidade Federal do Rio Grande do Norte, Caixa Postal 1641, 59072-970 Natal, Brazil.

[1] P. Grünberg, R. Schreiber, Y. Pang, M. O. Brodsky, and H. Sowers, Phys. Rev. Lett. **57**, 2442 (1986).

[2] M. N. Baibich, J. M. Broto, A. Fert, F. Nguyen Van Dau, F. Petroff, P. Etienne, G. Creuzet, A. Friederich, and J. Chazelas, Phys. Rev. Lett. **61**, 2472 (1988).

[3] S. S. P. Parkin, N. More, and K. P. Roche, Phys. Rev. Lett. **64**, 2304 (1990).

[4] M. Ruhrig, R. Shafer, A. Hubert, R. Mosler, J. A. Wolf, S. Demokritov, and P. Grünberg, Phys. Status Solidi A **125**, 625 (1991).

[5] U. Köbler, K. Wagner, R. Wiechers, A. Fuss, and W. Zinn, J. Magn. Magn. Mater. **103**, 236 (1992).

[6] W. J. Gallagher, S. S. P. Parkin, Yu Lu, X. P. Bian, A. Marley, K. P. Roche, R. A. Altman, S. A. Rishton, C. Jahnes, T. M. Shaw, and Gang Xiao, J. Appl. Phys. **81**, 3741 (1997).

[7] J. M. Daughton, J. Appl. Phys. **81**, 3758 (1997).

[8] B. A. Gurney, V. S. Speriosu, D. R. Wilhoit, H. Lefakis, R. E. Fontana, Jr., D. E. Heim, and M. Dovek, J. Appl. Phys. **81**, 3998 (1997).

[9] S. M. Rezende, C. Chesman, M. A. Lucena, A. Azevedo, F. M. de Aguiar, and S. S. P. Parkin, J. Appl. Phys. (to be published).

[10] A. Azevedo, C. Chesman, S. M. Rezende, F. M. de Aguiar, X. Bian, and S. S. P. Parkin, Phys. Rev. Lett. **76**, 4837 (1996).

[11] S. M. Rezende, M. A. Lucena, F. M. de Aguiar, A. Azevedo, C. Chesman, P. Kabos, and C. E. Patton, Phys. Rev. B **55**, 8071 (1997).

[12] M. A. Lucena, F. M. de Aguiar, S. M. Rezende, A. Azevedo, C. Chesman, and S. S. P. Parkin, J. Appl. Phys. **81**, 4770 (1997).

[13] B. Dieny and J. P. Gavigan, J. Phys.: Condens. Matter **2**, 187 (1990); W. Folkerts, J. Magn. Magn. Mater. **94**, 302 (1991).

[14] M. Maccio and M. G. Pini, Phys. Rev. B **49**, 3283 (1994); N. S. Almeida and D. L. Mills, *ibid.* **52**, 13 504 (1995); H. J. Elmers, G. Liu, H. Fritzche, and U. Gradmann, *ibid.* **52**, R696 (1995).

[15] T. L. Fonseca and N. S. Almeida, Phys. Rev. B **57**, 76 (1998).

[16] M. Schafer, S. Demokritov, S. Müller-Pfeiffer, R. Schafer, M. Schneider, P. Grünberg, and W. Zinn, J. Appl. Phys. **77**, 6432 (1995).

[17] P. Grünberg, S. Demokritov, A. Fuss, M. Vohl, and J. A. Wolf, J. Appl. Phys. **69**, 4789 (1991).

[18] A. Fuss, S. Demokritov, P. Grünberg, and W. Zinn, J. Magn. Magn. Mater. **103**, L211 (1992).

[19] R. J. Hicken, C. Daboo, M. Gester, A. J. R. Ives, S. J. Gray, and J. A. C. Bland, J. Appl. Phys. **78**, 6670 (1995).